



Active antibiotic resistome in soils unraveled by single-cell isotope probing and targeted metagenomics

Hong-Zhe Li^a, Kai Yang^a, Hu Liao^{a,b}, Simon Bo Lassen^c, Jian-Qiang Su^a, Xian Zhang^a, Li Cui^{a,1}, and Yong-Guan Zhu^{a,d,1}

Edited by Julian Davies, University of British Columbia, Vancouver, Canada; received January 27, 2022; accepted August 30, 2022

Antimicrobial resistance (AMR) in soils represents a serious risk to human health through the food chain and human–nature contact. However, the active antibiotic-resistant bacteria (ARB) residing in soils that primarily drive AMR dissemination are poorly explored. Here, single-cell Raman-D₂O coupled with targeted metagenomics is developed as a culture-independent approach to phenotypically and genotypically profiling active ARB against clinical antibiotics in a wide range of soils. This method quantifies the prevalence (contamination degree) and activity (spread potential) of soil ARB and reveals a clear elevation with increasing anthropogenic activities such as farming and the creation of pollution, thereby constituting a factor that is critical for the assessment of AMR risks. Further targeted sorting and metagenomic sequencing of the most active soil ARB uncover several uncultured genera and a pathogenic strain. Furthermore, the underlying resistance genes, virulence factor genes, and associated mobile genetic elements (including plasmids, insertion sequences, and prophages) are fully deciphered at the single-cell level. This study advances our understanding of the soil active AMR repertoire by linking the resistant phenome to the genome. It will aid in the risk assessment of environmental AMR and guide the combat under the One Health framework.

antimicrobial resistance | single-cell Raman | targeted metagenomics | risk assessment

Antimicrobial resistance (AMR) is recognized as one of the top 10 threats to global public health by the World Health Organization (1). The spread of AMR among humans, animals, and environments greatly promotes its prevalence and exacerbates the global One Health burden (2). Soil is an important interface that connects One Health sectors and represents the most significant but underexplored reservoir of AMR (3, 4). Anthropogenic activities such as manure application have induced blooms of antibiotic-resistant bacteria (ARB) and antibiotic-resistance genes (ARGs) in soils by directly transferring or exerting selective pressures (5–7). The accumulated AMR in soils could be reintroduced into humans via agricultural products and impact human health if transferred to human pathogens (8, 9). Soil microorganisms, which are the most enormous and diverse microbial consortia on Earth (10), play a key role in populating and spreading AMR. The active cell fractions are even more critical in contributing to these processes (11). However, because the large majority of microbes are yet uncultured, and this ratio is even up to 99% in soils (12, 13), understanding the indigenous active ARB in soils and pinpointing “who is doing what and how” remains a major challenge, hindering the combat against this global AMR threat.

Metagenomic sequencing and high-throughput (HT) PCR have greatly enhanced our knowledge of the soil microbiome and resistome by producing a wealth of gene sequence-based information (6, 7, 14). However, genomic information represents only inferred rather than real AMR capabilities (15). Moreover, genotypic analysis cannot always differentiate the genes derived from extracellular DNA, dead, or active cells, which significantly impact the risks associated with acquiring and spreading the AMR. Previous work reported that 40% of microbial diversity in soil on average was derived from dead cells or extracellular DNA, leading to misestimations of taxa related to key soil processes (6, 16). These relic DNA may also contribute to the soil resistome. Furthermore, a large fraction of microbes, ~80% or more, were demonstrated to be dormant in soils (17). Therefore, linking the soil AMR level and risk to only genotypic information is not enough, and phenotypic information should also be included. Traditional culture-based methods can characterize phenotypic AMR traits, i.e., observing the bacterial growth in the presence of antibiotics (5). However, focusing only on a limited number of culturable indicator bacteria neglects the large majority of intrinsic soil microbes, especially the uncultured fraction that may exist as a dominant AMR pool (12). Therefore, cutting-edge approaches are essential for deciphering the previously underexplored ARB in soils, evaluating the phenotypic resistance levels, and elucidating the underlying genetic determinants.

Significance

Measuring active cells that contribute to soil antimicrobial resistance (AMR) is critical for understanding AMR behavior in ecosystems. Here, single-cell Raman with isotope labeling was developed to profile active antibiotic-resistant bacteria (ARB) inhabiting different soils. Their abundance and activity in soils increased with anthropogenic activities. Further targeted single-cell sorting and metagenomics pinpoint “who is doing what and how” in the most active ARB. Several uncultured genera and a pathogenic strain were identified, along with the underlying resistance genes and mobile genetic elements. This approach linking the resistant phenome to the genome is highly valuable for assessing AMR risk and in guiding human activities against AMR.

Author affiliations: ^aKey Laboratory of Urban Environment and Health, Fujian Key Laboratory of Watershed Ecology, Institute of Urban Environment, Chinese Academy of Sciences, Xiamen 361021, China; ^bUniversity of the Chinese Academy of Sciences, Beijing 100049, China; ^cDepartment of Plant and Environmental Sciences, Faculty of Science, University of Copenhagen, 1871 Frederiksberg, Denmark; and ^dState Key Laboratory of Urban and Regional Ecology, Research Center for Eco-Environmental Sciences, Chinese Academy of Sciences, Beijing 100085, China

Author contributions: L.C. and Y.-G.Z. designed the study; H.-Z.L. and K.Y. performed research; L.C. and X.Z. contributed new analytic tools; H.-Z.L., H.L., and L.C. analyzed data; and H.-Z.L., S.B.L., J.-Q.S., L.C., and Y.-G.Z. wrote the paper.

The authors declare no competing interest.

This article is a PNAS Direct Submission.

Copyright © 2022 the Author(s). Published by PNAS. This article is distributed under [Creative Commons Attribution-NonCommercial-NoDerivatives License 4.0 \(CC BY-NC-ND\)](https://creativecommons.org/licenses/by-nc-nd/4.0/).

¹To whom correspondence may be addressed. Email: lcui@iue.ac.cn or ygzhu@cees.ac.cn.

This article contains supporting information online at <http://www.pnas.org/lookup/suppl/doi:10.1073/pnas.2201473119/-DCSupplemental>.

Published September 26, 2022.

Single-cell Raman spectroscopy coupled with heavy-water labeling (Raman-D₂O) is an appealing metabolic activity-based approach for discerning the phenotype of ARB in a culture-independent way (18–23). When incubated with heavy water, metabolically active cells can assimilate ²D via de novo synthesis into cellular biomolecules, thus generating a new C-D band that can be specifically detected by Raman spectroscopy (19, 24). Under antibiotic treatment, antibiotic-resistant (R) and sensitive (S) cells display distinct metabolic activities toward D, enabling the use of C-D band in a simple and even quantitative manner to discriminate R/S and evaluate the resistance levels (20, 21). Raman-D₂O has shown consistent results with conventional culture-based methods in determining the R/S of clinical bacterial isolates (20). When extrapolating to environments, heavy-water amendment has an additional advantage of exerting no alteration on the substrate pool; moreover, the non-invasive nature of Raman spectroscopy further allows targeted sorting and sequencing of cells to unravel the underlying genetic determinants (25–29). Raman-D₂O has been employed to detect ARB in river water and human gut (28, 29). However, its use in soil resistant microbiota has never been explored. Soil is a much more complex matrix in which microbes are dispersed in a large background of abiotic particles that may significantly impact antibiotic efficiency, microbial heavy-water assimilation, and consequently efficient application.

Here, single-cell Raman-D₂O with targeted metagenomics was developed as a culture-independent functional assay to elucidate the active soil antibiotic resistome. It provides a measure of both phenotype and genotype of indigenous ARB in soils not previously captured by conventional molecular methods. Comparative analysis of the abundance and activity of ARB in three different anthropogenically impacted soils was performed. Through further targeted single-cell sorting and metagenomic sequencing of the most active ARB, comprehensive genotypic information underlying the resistant phenotype was revealed, including taxa, ARGs, virulent factor genes (VFGs), and mobile genetic elements (MGEs). This study takes the investigation of AMR a large step further by deciphering soil active AMR pools. This multipronged approach can be broadly applied to other ecosystems to gain an in-depth understanding of environmental AMR, aid risk assessment, and promote strategies against the global AMR threat.

Results and Discussion

Efficiency of Antibiotics in Inhibiting the Activity of Native Soil Microbiota. To optimize the Raman-D₂O approach for soil resistant microbiota, the incubation time and antibiotic efficiency in soils were firstly examined. The appropriate incubation time was determined by amending two types of farmland soils with or without manure application with 20% D₂O (v/w) and incubating at 27 °C for 0, 12, 24, and 36 h. Subsequently, soil microorganisms were extracted for single-cell Raman measurement (30). Fig. 1A shows the typical Raman spectra from individual soil bacteria. The spectral features differed dramatically, indicating the high diversity of soil microbes in cellular composition and physiology. Some bacteria were observed to show a C-D band at 2,040–2,300 cm⁻¹ (red line), demonstrating that they actively assimilated D₂O-derived D into cellular components such as lipids and proteins. C-D ratios (CD/[CD+CH]) derived from ~50 individual bacteria at each sampling time were used to represent the D incorporation level (19). As shown in Fig. 1B, the ratios from both soils increased over time until reaching a plateau at 24 h, and no significant

increase was observed at 36 h. Therefore, 24 h was chosen as the appropriate time for labeling native soil microbes considering effective D labeling and meanwhile minimizing the potential impact on soil microbial community. We noticed that the C-D ratios in manured farmland soils (MFS) were higher than those in farmland soils (FS). This is likely related to the higher concentration of Olsen P and dissolved organic carbon (DOC) in MFS relative to FS (*SI Appendix*, Fig. S1). These nutrients have been previously demonstrated to enhance soil microbial activities toward D uptake (30).

The key to R/S discrimination by Raman-D₂O lies in the distinct metabolic activities of these microorganisms against antibiotic treatments. However, soil matrices have been indicated to impact the efficiency of amended antibiotics via adsorption or degradation (31). For example, β-lactam and quinolone antibiotics can tightly adsorb to soil particles (31), thereby reducing their inhibiting effects on microbial activity. Therefore, proper doses of antibiotics must be applied to soil to maintain sufficient bioavailable concentrations for efficient activity inhibition and ARB discrimination. Here, antibiotics with application doses ranging widely from 1× to 100× the Clinical and Laboratory Standards Institute minimum inhibitory concentration [CLSI MIC (32)] were introduced to soils in the presence of D₂O for 24 h. Considering that soil microbes with clinically relevant resistance would pose a higher risk to human health, three clinically important antibiotics with different antibacterial mechanisms were used, including meropenem (last-resort antibiotic), ciprofloxacin (quinolones), and cefotaxime (third-generation cephalosporin). Both meropenem and cefotaxime inhibit cell wall synthesis, while ciprofloxacin inhibits bacterial DNA synthesis. The dose-dependent C-D ratios in each treatment are shown in Fig. 1C. To eliminate the effects of soil nutrition levels on the D incorporation level, C-D ratios were all normalized with the control from antibiotic-free soils. The threshold for considering a cell actively labeled was determined at 0.5 by calculating the mean + 3× SD of normalized C-D ratios in bacteria without D labeling (19, 33).

A broad distribution of C-D ratios was observed, indicating the highly heterogeneous metabolic activities of soil microbes in response to antibiotics. With the increase of the applied antibiotic dose, the activities of soil bacteria were inhibited as observed from the declining ratios. The inhibitory effect was not the same for the three antibiotics. For meropenem, a significant decrease was observed at 10× and 100× MIC ($P < 0.001$), with the percentage of active cells declining to 24.2% and 11.7% respectively in comparison with the 86.5% at control. This result indicated that only a small fraction of cells in soils can tolerate such high doses of meropenem and maintain their activity. Similar phenomena were observed in the cefotaxime treatment, with the percentage of active cells declining to 29.1% and 27.2% at 10× and 100× MIC, respectively. By comparison, for ciprofloxacin, a significant decrease in C-D ratios in both soils occurred only at 100× MIC ($P < 0.001$) with a much higher percentage of active cells (53.4%). Clearly, the applied antibiotic doses of 10–100× MIC that can inhibit the in situ metabolic activity of bacteria in soils were much higher than those used in clinical strains (20). Although the complex soil matrix reduced the antibiotic efficiency, the application of a proper dose was still enough to screen the active cells in native soils. The contrasting inhibitory effect of antibiotics on soil microbes could be due to two reasons. One is related to the distinct adsorption behaviors of antibiotics on soil aggregates (31, 34). For example, ciprofloxacin was reported to be more easily absorbed onto soil particles than

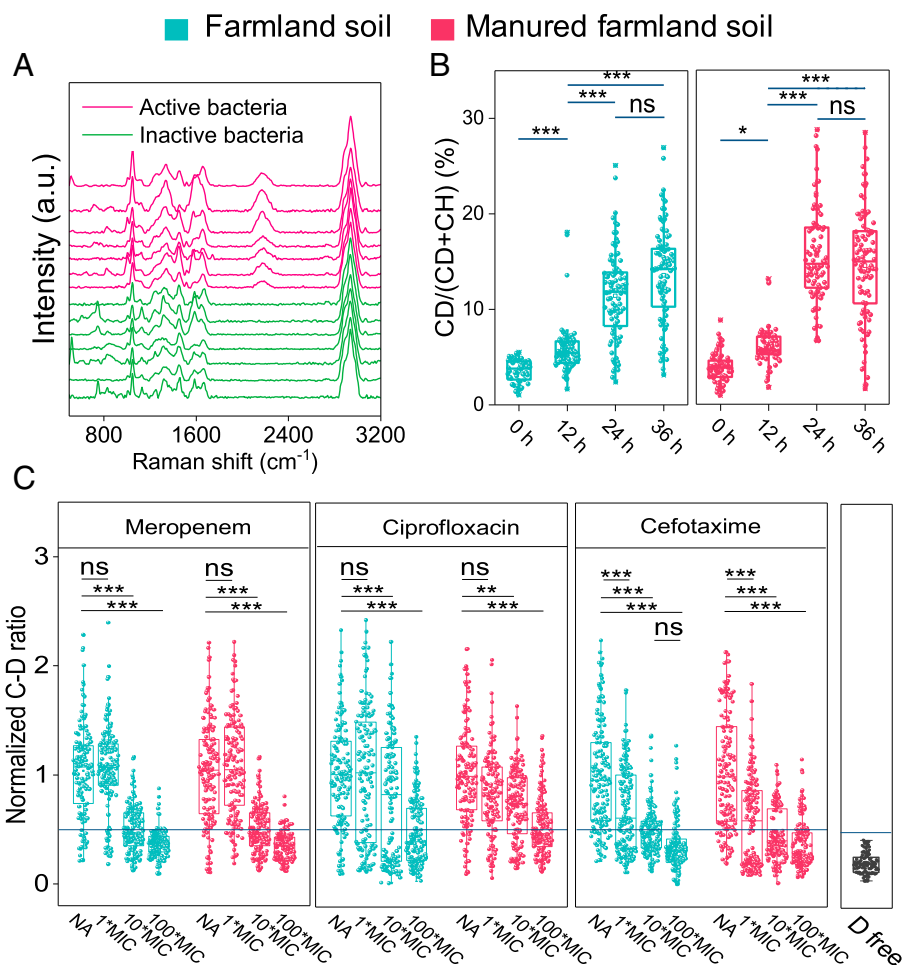


Fig. 1. Efficiency of antibiotics in inhibiting activity of native soil microbiota. (A) Raman spectra of individual soil bacterium incubated with 20% (v/w) D₂O amended to soils for 24 h. The red and green spectra represent active bacteria with C-D band and inactive bacteria without C-D band, respectively. (B) Time-dependent C-D ratios (CD/(CD + CH) (%)) of soil bacteria incubated with D₂O. (C) Dose-dependent normalized C-D ratios of soil bacteria amended with 0, 1x, 10x, and 100x CLSI MIC of meropenem, ciprofloxacin, and cefotaxime, respectively. Normalized C-D ratios are calculated by dividing C-D ratios of individual soil bacterium from antibiotics-amended soils by the average C-D ratio from antibiotic-free soils. The blue line represents the threshold value to distinguish active and inactive cells. It is determined as the mean + 3xSD of cell without D₂O addition (D free). The asterisk on the columns represents significance (**P* < 0.05; ***P* < 0.01; ****P* < 0.001, ns, no significant difference, via one-way ANOVA).

meropenem and cefotaxime, partly explaining the higher concentration of ciprofloxacin required to effectively inhibit microbial metabolism (34). The other reason may be associated with the varying phenotypic resistance levels of soil intrinsic bacteria to different antibiotics.

Development of Raman-D₂O for Identifying Soil Active ARB.

Because the soil microbiota studied above contains a hybrid of antibiotic-resistant and sensitive bacteria, without a clear R/S cutoff value, it is still not possible to discriminate ARB in soils. To solve this problem, three resistant strains against meropenem (Mero^r, *Chryseobacterium indologenes* pq15-1), ciprofloxacin (Cip^r, *Diaphorobacter* sp. SL205), and cefotaxime (Cef^r, *Chryseobacterium gleum* 19) were isolated from the farmland soil. Together with two typical antibiotic sensitive gram-negative bacteria (*Escherichia coli* DH5α) and gram-positive bacteria (*Staphylococcus aureus* RN4220), all bacteria were transplanted into sterilized soils (FS and MFS) amended with 0, 1x, 10x, and 100x CLSI MIC of antibiotics respectively. After following the same incubation and extraction procedure as that of the native soil bacteria, single-cell Raman spectra of the inoculated bacteria were measured, and their normalized C-D ratios are shown in Fig. 2. The distribution of C-D ratios from the single inoculant was accordingly much narrower than that from

soil microbiota containing diverse microbes. More interestingly, the inhibitory effects of three antibiotics on antibiotic sensitive and resistant inoculates were totally different. For the two sensitive *E. coli* and *S. aureus* strains in both types of soils, significant activity inhibition was observed at meropenem/cefotaxime of ≥10x MIC and ciprofloxacin of 100x MIC (Fig. 2 A and B). Such inhibition doses were similar to those of the soil microbial consortia, which also exhibited the lowest decline in activity with the addition of ciprofloxacin (Fig. 1C). In contrast, for the three ARB isolated from and then reintroduced to soils, nearly all maintained high activities against the three antibiotics except the 100x MIC meropenem (Fig. 2C). Such contrasting activity of R and S in response to antibiotics indicated the feasibility of discerning native ARB in soils by Raman-D₂O. Here, by taking soil types, antibiotic types, and discrimination sensitivity all into account, antibiotic doses of 10x MIC of meropenem/cefotaxime and 100x MIC of ciprofloxacin were determined as the proper applied dose, and the highest normalized C-D ratio of 0.5 that antibiotic sensitive strains can reach was set as the R/S threshold value.

The bacterial community structures of each soil before and after amendment with the abovementioned antibiotics at the determined doses were further compared by 16S rRNA gene amplicon sequencing. The principal coordinates analysis

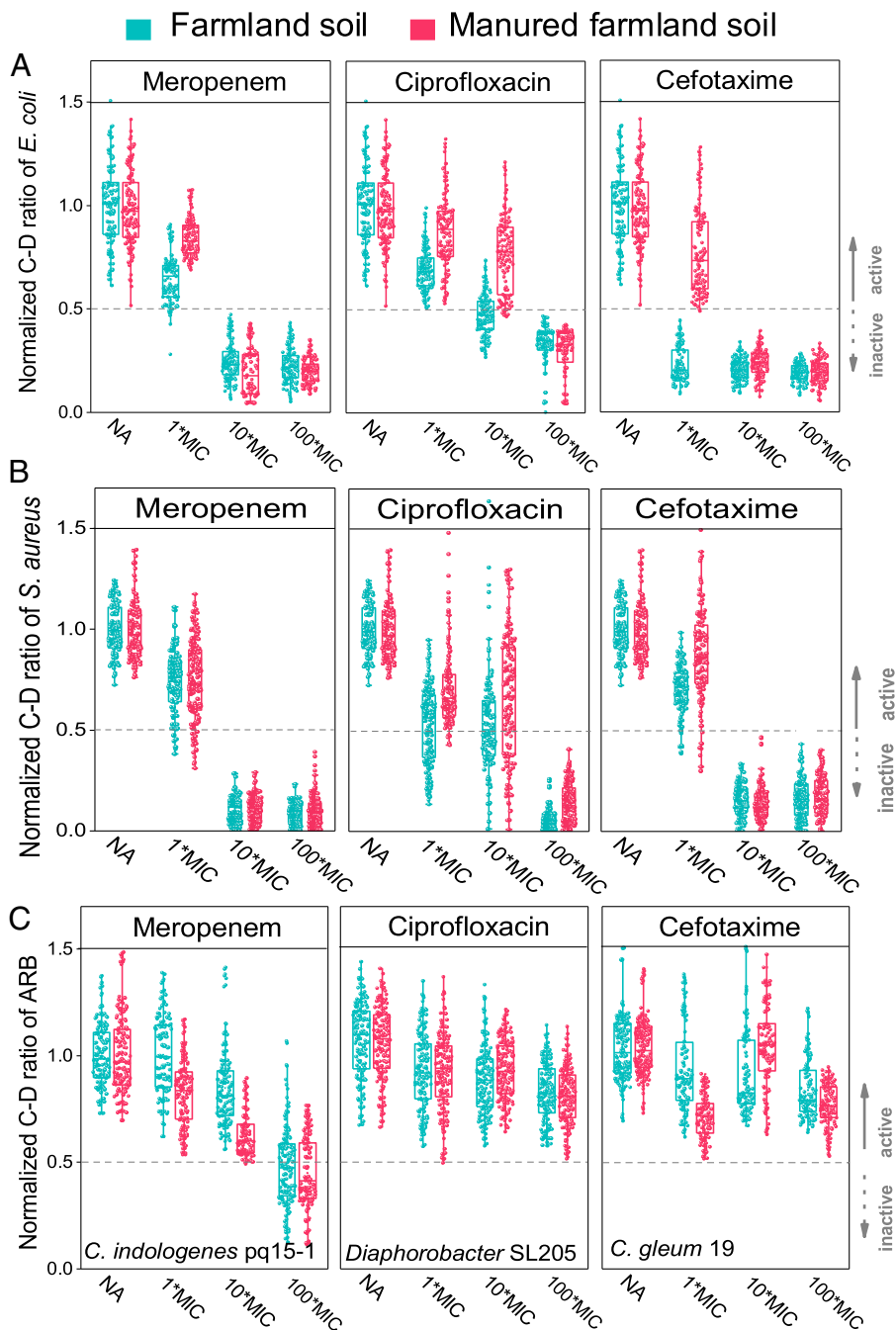


Fig. 2. Development of Raman-D₂O for soil active ARB identification. The normalized C-D ratios of two antibiotic sensitive bacteria of (A) *E. coli*, (B) *S. aureus*, and (C) three ARB isolated from soils incubated in farmland soil and MFS amended with 0, 1×, 10×, and 100× CLSI MIC of meropenem, ciprofloxacin, and cefotaxime, respectively. The gray dotted line represents the threshold value for distinguishing R/S cells.

(PCoA) plot based on the Bray-Curtis dissimilarity metrics revealed no significant shift (Adonis test, $P > 0.05$, *SI Appendix*, Fig. S2), indicating that the soil bacterial communities did not change after 24 h incubation with the added three antibiotics, consistent with a previous study (35). This ensured the reliable application of Raman method in assessing the phenotypic resistance of soil microbial communities.

Taken together, by fully evaluating multiple potential effects, including incubation time, antibiotics application dose, R/S cutoff value, soil and bacterial types, a culture-independent single-cell Raman-D₂O strategy for studying active ARB in soils was developed. Presently, phenotypic resistance is primarily studied by culture-based methods and interpreted according to the clinical breakpoints (e.g., MIC or inhibition zone) from

the CLSI or the European Committee on Antimicrobial Susceptibility Testing (6). However, they are only applicable to culturable pathogenic bacteria, but not to the vast majority of unculturable environmental microorganisms, and there is currently no standard resistance testing method for environmental microbiota. Here, the established Raman-D₂O approach and interpretation threshold enable the elucidation of environmental ARB which represent an important reservoir of AMR.

Evaluation of Phenotypic AMR Level in Soils. Risk assessment of AMR is a strategic priority for public health. It is currently based primarily on genetic information, but is limited by the lack of its phenotype data (36). In this work, by using the established Raman-D₂O, both the percentage of ARB in soils

■ Tibetan soil ■ Farmland soil ■ Manured farmland soil

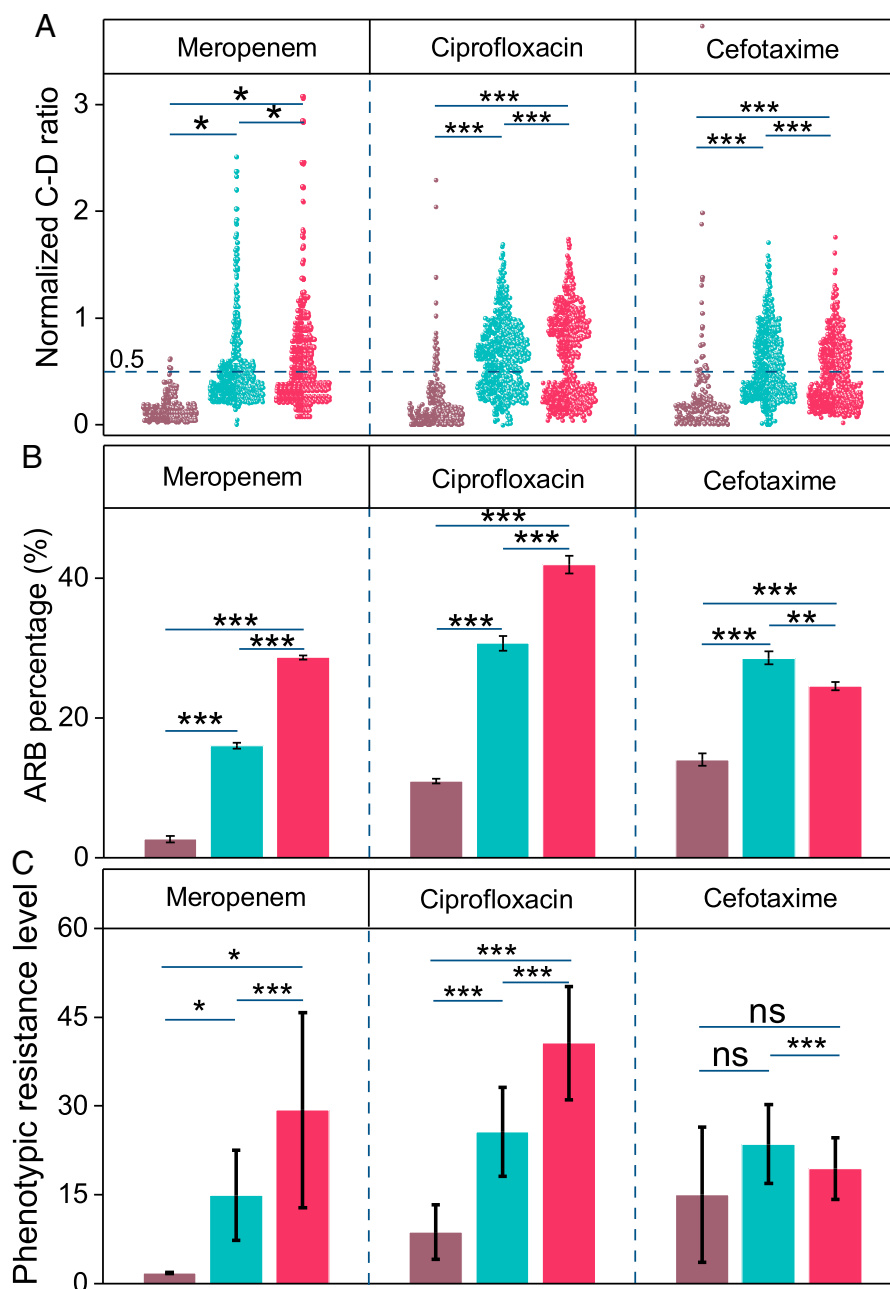


Fig. 3. Evaluation of phenotypic antibiotic resistance level of soils. The normalized C-D ratios (A), ARB percentage (B), and phenotypic resistance level (C) against antibiotics of meropenem, ciprofloxacin, and cefotaxime in Tibet soil, farmland soil, and MFS, respectively. The gray dotted line in A represents the threshold value for distinguishing R/S cells.

and their activities against antibiotic treatment can be quantified. Compared with chemical contaminants that will degrade in environment over time, ARB and the harbored ARGs are biological contaminants that can proliferate, spread and persist in environments. Moreover, active ARB probably contribute more to AMR behaviors than dominant and dead cells in ecosystems (37). The ARB abundance (percentage) was calculated as the number of active ARB divided by the total number of bacteria measured by single-cell Raman spectroscopy. Because of the high diversity and abundance of soil microbes, the balance between statistical power and time cost should be considered when determining the number of Raman-measured cells required to obtain a representative percentage of soil ARB. Here, more than 600 single cells in each antibiotic treatment

(a total of ~4,000 cells) were detected by single-cell Raman spectroscopy and a total of 200 random single-cell samplings under each bacterial count were employed to calculate the percentage of ARB (*SI Appendix, Fig. S3*). As the number of detected cells increased, the variation in the ARB percentage declined and stabilized. To determine the proper cell number, a Boltzmann function was nonlinearly fitted to the upper bound of the ARB percentage (red curve in *SI Appendix, Fig. S3*). The results showed that the derivative of each function became zero when the number of cells exceeded 150. Hence, 150 cells were determined as the minimum number to reliably determine ARB percentage in soils.

ARB in three soils with different anthropogenic impacts were studied, including one pristine soil from an unpopulated zone in Tibet (TS), and two farmland soils (FS and MFS). Fig. 3A

shows the distribution of normalized C-D ratios in each native soil against three antibiotics. Significant differences among three soil types were observed ($P < 0.05$). The percentages of active ARB against all three antibiotics in the two farmland soils (16.1–41.9%) were significantly higher than in Tibet soils (2.7–14.1%, $P < 0.05$) (Fig. 3B). The application of manure further increased the abundance of *mero^r* (from 16.1 to 28.6%) and *cip^r* (from 30.6 to 41.9%) in farmland soils, while a slight decline (from 28.5 to 24.6%, $P < 0.05$) was observed for *cef^r*. These findings clearly indicated that anthropogenic manure induced the increase of ARB in the soil microbiota, consistent with previous works showing that human activities such as animal farming, manure fertilization, and wastewater reclamation enriched AMR through direct release or selection (5, 7, 38). Of note, although there are nearly no human activities in the soil from the Tibet depopulated zone, a low portion of active ARB were still observed. The reason is likely related to the ancient feature of AMR in microbes, which is naturally widespread in environments regardless of human influences (39). Additionally, bacteria resistant to the last-resort meropenem exhibited the lowest abundance among three antibiotics in nearly all three soils ($P < 0.05$). This result could be related to that meropenem is cautiously prescribed to treat severe infections (40), while ciprofloxacin and cefotaxime are more widely used in treating urinary and respiratory tract infections (41).

Some soil ARB exhibited remarkably high metabolic activities (Fig. 3A) and thus may contribute more to AMR dissemination via horizontal gene transfer (HGT), mutation, proliferation, or in combination (6, 37). Here, the percentage of ARB and their activities were multiplied to represent the phenotypic AMR level of soils. The obtained phenotypic levels displayed a similar trend to that of ARB percentage but were more variable due to the highly varying activities of soil ARB (Fig. 3C). Genotypic resistance levels of soils were also evaluated here by measuring the abundance of ARGs encoding resistance to the three antibiotics by HT qPCR (*SI Appendix, Fig. S4*). As expected, the trend of genotypic resistance was not entirely consistent with that of phenotypic resistance. For instance, no differences in the abundance of carbapenem and β -lactam ARGs between MFS and FS were observed. Only the abundance of fluoroquinolone ARGs displayed a higher level in MFS than FS ($P < 0.05$), which was similar to that observed for the phenotype. Several reasons could explain this difference. First, DNA from dead/dominant cells and extracellular DNA contributed to the detected ARGs. A recent study reported that up to 40% of soil microbial diversity retrieved through genomic sequencing could come from dead cells (16). Second, some ARGs harbored by soil microbes may not be expressed. Third, unknown or novel ARGs in soils cannot be targeted by HT-qPCR.

Overall, this work established a phenotypic AMR level based on the abundance and activities of ARB in native soils screened

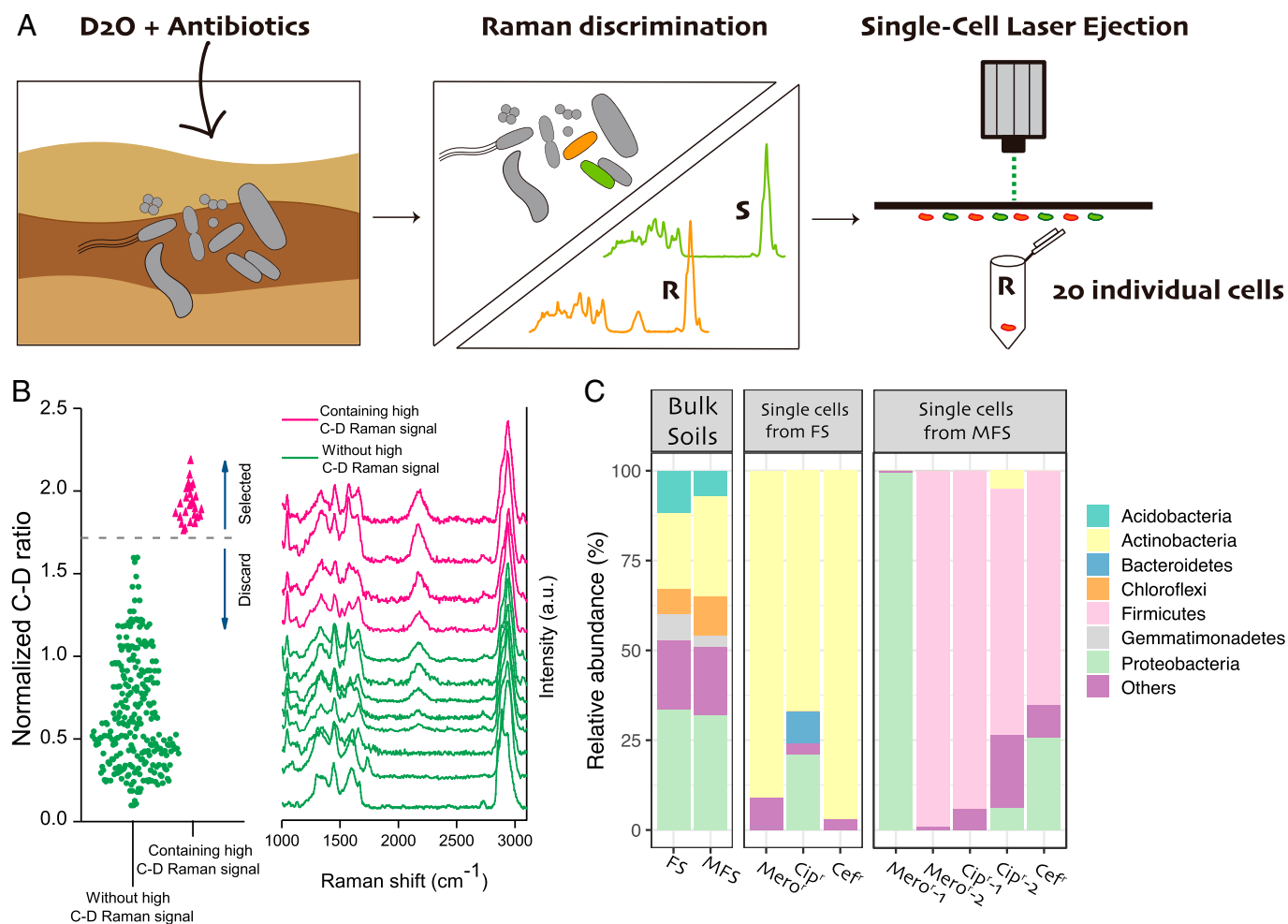


Fig. 4. Single-cell capturing and sequencing of active ARB in soils. (A) Workflow for capturing highly active ARB from soils via targeted single-cell sorting. (B) Active ARB with normalized C-D ratios > 1.6 (top 2%, red dots) were selected for sorting (Left). Representative single-cell Raman spectra of highly active bacteria (red line) and less active or dormant bacteria (green line) (Right). (C) Relative abundance of dominant phyla in bacterial communities of bulk soil (Left), the captured highly active ARB from farmland soils (Middle) and MFS (Right).

by single-cell Raman-D₂O. It constitutes an important risk factor that will aid risk assessment of AMR in environmental settings. Compared with genotypic resistance, phenotypic resistance is more associated with enhancing AMR spread and causing treatment failure. Therefore, an integrated risk assessment platform including both phenotypic and genotypic resistance will be invaluable in identifying environmental hotspots and regulating human practices for resistance control, such as soil fertilization with manure and wastewater reuse.

Single-Cell Capturing and Sequencing of Active ARB in Soils.

The noninvasive Raman detection method allows for targeted sorting and sequencing of soil ARB to decipher taxa and the underlying resistome, thereby enabling the linkage of the resistance phenotype to genotype. Here, single-cell laser ejection based on “point to point” laser-induced forward transfer was employed to sort out the most active ARB (Fig. 4A). Around 140 cells highly labeled by deuterium at the top 2% were sorted after each antibiotic incubation (Fig. 4B). Metagenomic sequencing of the sorted ARB revealed that Actinobacteria, Proteobacteria, and Firmicutes were the dominant phyla (Fig. 4C). All of them were found to be present in the metagenome of bulk soil communities. A total of 31 active ARB were identified from the sorted minimetagenome, representing only a minute fraction of the overall soil bacterial diversity (Fig. 5A). Among them, *g_Cutibacterium* was found in all three sorted groups of farmland soils. It is known as a human colonizer and is also generally found in soils (42). *Bacillus* was frequently detected in *cip*^r. It is a common genus in soil habitats and a fraction of *Bacilli* strains can cause ear infections and meningitis (43). Two potential pathogenic bacteria, *Haemophilus influenzae* and *Haemophilus parainfluenzae*, were identified in the *mero*^r of manured soil. Notably, in nearly all the sorted fractions, ARB affiliated with the uncultured genera were detected, including *Haemophilus*, *Streptococcus*, *Bacillus*, and *Cutibacterium*, indicating that the uncultured soil bacteria were important contributors to soil phenotypic resistance. All of these genera have been previously reported to have uncultured representatives in soils (20). However, their prevalence and contributions to AMR were previously seldom evaluated due to the lack of a phenotypic tool to investigate them in a culture-independent manner. In addition, we noticed that all the isolated individual ARB were at low abundance in the bulk soil communities (Fig. 5A). Similar phenomenon was found in fluorescence-activated cell sorting of cellulose-degrading bacteria in Great Boiling Spring, where the sorted fraction were uncovered from rare species. These findings demonstrate that single-cell approaches provide a way to study rare species (44). Despite the low abundance of ARB, the high metabolic activity under antibiotic treatment implied their potential role in spreading AMR and causing infections.

In addition to the taxonomic identity of the sorted ARB, genotypic information of ARGs underlying the phenotypic resistance was also deciphered in order to provide an in-depth understanding of AMR. A total of 12 ARG subtypes were identified in the sorted resistant fractions from the two farmland soils (Fig. 5B and *SI Appendix*, Table S1). These ARGs were well correlated with the phenotypic resistance. For example, in the sorted *cip*^r fraction, quinolone resistance genes of *gyrA* and efflux pump genes of *bcrA* and *oleC* were detected. In the sorted *cef*^r fraction, beta-lactam resistance genes of PBP and efflux pump genes of *macB*, *novA*, *msbA*, and *bcrA* encoding multidrug resistance were detected. In the *mero*^r fraction, a more diverse ARGs were detected, including genes encoding resistance

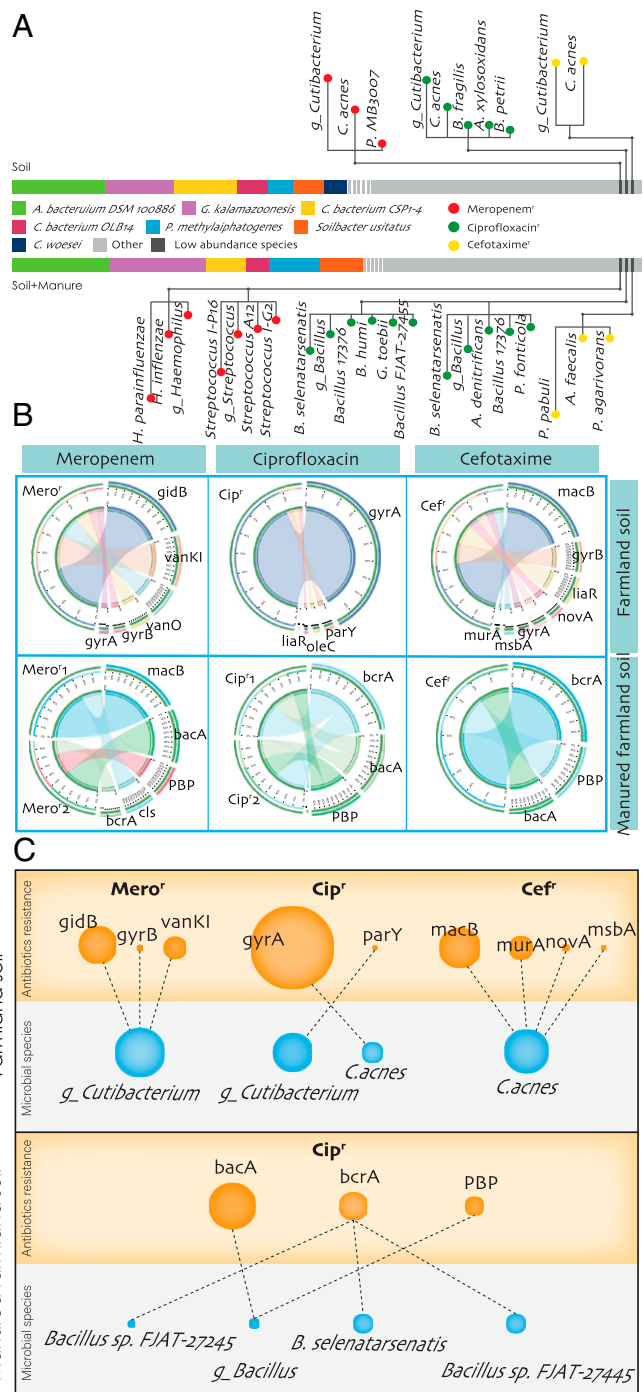


Fig. 5. Targeted minimetagenomics of active ARB from soil microbiota. (A) The composition and relative abundance of bulk soil bacterial communities before sorting and the recovered taxa of highly active ARB after sorting. (B) The diversity and abundance of detected ARGs in the captured soil ARB. The width of inner ribbon represents the relative abundance of ARGs in the captured bacteria. (C) Distribution of ARGs in the sorted active soil ARB host. The area of the circles represents the abundance of bacteria and ARGs detected in the database.

to multidrug (*macB* and *bcrA*), vancomycin (*vanK1*, *vanO*), aminoglycoside (*parY*, *gidB*), and fluoroquinolone (*gyrA*, *gyrB*). Meropenem is the last-resort antibiotics. The cooccurrence of multiple ARGs in the *mero*^r was consistent with previous findings in meropenem-resistant bacteria isolated from hospital effluents that exhibited resistance to more than 12 antibiotics (45). By further analyzing the cooccurrence of ARGs and taxonomic marker genes in individual contigs, the taxonomic distribution

of ARGs in eight sorted bacteria was determined (Fig. 5C). Some ARB such as *Cutibacterium acnes* (*C. acnes*) and *g_Cutibacterium* were found to harbor 3–4 types of ARGs and virulence factor genes (SI Appendix, Fig. S5), raising health concerns on these multidrug-resistant pathogens. Remarkably, three uncultured bacteria of *g_Cutibacterium* and *g_Bacillus* were found to carry 1–3 types of ARGs, confirming the substantial contribution of the large majority of uncultured bacteria to soil AMR reservoirs. Moreover, the most abundant taxa (e.g., *g_Cutibacterium*) were not the host harboring the most abundant ARGs, and vice versa (e.g., *C. acnes*), suggesting that a certain ARB tended to associate with more ARGs (Fig. 5C).

Finally, one ARGs-carrying metagenome-assembled genome (MAG) was successfully retrieved from the sorted minimetagenome via sequence binning analysis. Genomic quality estimation indicated that the completeness and contamination were 50.0% and <5% respectively (SI Appendix, Table S2). Phylogenomic reconstruction annotated the MAG to *C. acnes* by placing its MAG into the phylogenetic context of 27 known *C. acnes* strains with a complete genome (Fig. 6A). Compared with the ARGs (4) and VFGs (36) reported in the known *C. acnes* strains isolated mainly from clinical settings (SI Appendix, Table S3), three

ARGs (*sul3*, *vmlR*, *vanHO*), and 3 VFGs (*flmH*, *pknG*, *hisF*) were uniquely detected in this soil-derived MAG here (Fig. 6A), indicating that it is a novel strain. The reason could be related to the exchange of genetic elements between *C. acnes* and other soil-inhabiting microbes via HGT. For example, the plasmid fragments may create an ideal condition allowing ARGs and VFGs to be recruited and accumulated through recombination. Additionally, genetic context around ARGs and VFGs that affected transmission and virulence potential was studied by analyzing contigs containing MGEs, ARGs, and VFGs (Fig. 6B). Many types of insertion sequences (IS) were detected on the contigs together with multiple ARGs and VFGs. For example, contig 29 carried 1 IS fragment (IS 21), 2 ARGs (*macB*, *VanK1*), and 3 VFGs (*katA*, *hmuU*, *devR*); contig 30 contained 1 IS fragment (IS 481), 1 ARG (*teB*), and 5 VFGs (*pgi*, *mprA*, *ptpA*, *cfa*, *pdhB*). Of note, prophage and IS displaying a mosaic distribution were detected on a conjugative plasmid on contig 48 (Fig. 6B). Although ARGs carried on IS cannot move intercellularly, they can hitch onto intercellular mobile elements (e.g., plasmids) and become transferable, thereby increasing the possibility of HGT (46). According to a recent framework categorizing the risk of ARGs into four levels (36), these ARGs in MGEs harbored by pathogenic *C. acnes* can be ranked as the second highest risk. Additionally, the *C. acnes* was highly metabolically active in native soils, raising a further concern that they might actively spread ARGs and VFGs from the farmland soils to human pathogens. Collectively, Raman-based single-cell sorting and sequencing linked AMR phenotype with multiple genotypes (taxa, ARGs, VFGs, and MGEs). More strikingly, it provides answers to “who is doing what and how” for the uncultured soil ARB that were largely underexplored. However, the MAG that can be assembled from the sorted ARB was still very limited due to the potential damage of laser to the target bacteria (47, 48). This problem could be further improved by optimizing or developing new sorting methods.

In conclusion, we have established an approach to characterizing both phenotype and genotype of active ARB intrinsic in a wide range of soils. These active AMR pools are of particular concern because they mainly drive the AMR transmission but are largely underexplored. We clearly reveal an elevated level of abundance and activity of phenotypic ARB in anthropogenically impacted soils. The phenotypic resistance obtained here constitutes a factor that will aid risk assessment of environmental AMR. Moreover, targeted sorting and metagenomic sequencing of the most active ARB in soils lead to the identification of several uncultured bacterial genera and a pathogenic strain, together with the underpinning genetic elements including ARGs, plasmids, IS, and phages. This work advances our understanding of soil active AMR pool. This approach can be broadly extended to other ecosystems and is highly valuable for identifying environmental hotspots, regulating human practices, and developing policies to combat AMR under the One Health framework.

Materials and Methods

Bacterial Strain and Antibiotics. The bacteria used in this study included mero^r *C. indologenes* pq15-1, cip^r *Diaphorobacter* sp. SL205, cef^r *C. gleum* 19 isolated from soils, and antibiotic-sensitive *E. coli* DH5 α and *S. aureus* RN4220 purchased from Guangdong Microbial Culture Collection Center. The MIC of antibiotic-sensitive bacteria are shown in SI Appendix, Table S4. The antibiotics used in this study included meropenem (Target Molecule Corp., Boston, MA), ciprofloxacin (Macklin, Shanghai, China), and cefotaxime (Macklin, Shanghai, China). All the antibiotic solutions were sterile filtered through a 0.22 μ m filter

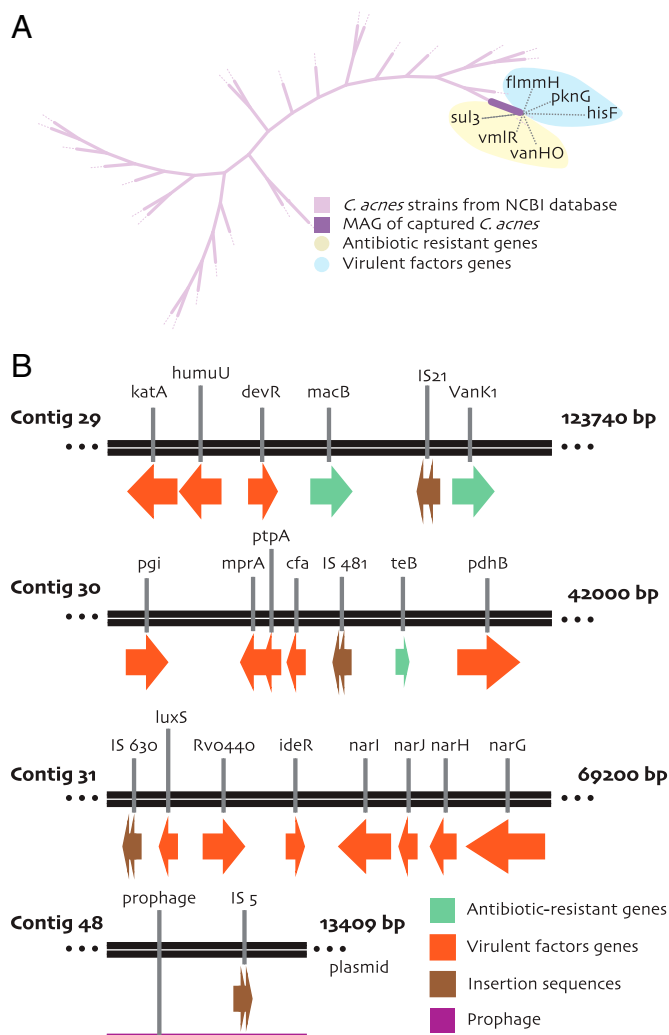


Fig. 6. Characterization of a pathogen MAG recovered from sequencing of sorted fractions. (A) Phylogenetic tree displaying the genotypic heterogeneity of *C. acnes* alongside their nearest neighbors based on BLAST searches against the NCBI database. The genes of captured *C. acnes* were shown with dark orchid branch. (B) Schematic of the genetic organization of ARGs, VFGs, and MGEs.

(Millipore Millex, USA), and stored at -20°C before use. The other chemicals were purchased from Sinopharm Chemical Reagent Company.

Soil Sample Collection and Properties Analysis. Soil samples were collected from a long-term field experiment station in Zhejiang province and one depopulated zone in Tibet, China respectively. Detailed information about the long-term field experiment is shown in *SI Appendix, Table S5*. Two treatments of no fertilization and manure fertilization were selected. The pristine soils from Tibet were collected from a depopulated zone at an altitude of 4,500 m. Soils were air dried at room temperature, then homogenized and sieved through a 0.6 mm sieve to remove stones. Sterilized soils were prepared by drying the soils in an oven at 120°C overnight. The soil DOC was measured by a TOC analyzer (TOC-LCPH, Shimadzu, Japan) at a soil-to-water ratio of 1:5 (wt/vol) (49). The soil Olsen P was extracted by 0.5 mol/L Na_2CO_3 and measured by molybdenum-blue colorimetric method (50).

Antimicrobial R/S Discrimination of Soil Bacteria via D_2O Labeling. Soil pellets were dried at 27°C for 16 h to remove extra moisture. For deuterium isotope labeling, 1 g of the as-prepared soils were amended with 200 μL of D_2O (99% atom % D, Sigma-Aldrich) and incubated at 27°C . To determine the appropriate soil incubation time, soil samples were collected at 0, 12, 24, and 36 h to test the D incorporation levels of soil microorganisms. To determine the appropriate concentrations of antibiotics to achieve R/S discrimination, original soils and sterilized soils inoculated with the abovementioned five antibiotic resistant and sensitive bacteria were all incubated with D_2O and 0, 1 \times , 10 \times , 100 \times CLSI MIC of meropenem, ciprofloxacin, and cefotaxime (*SI Appendix, Table S6*), respectively. The soil microorganisms were harvested via Nycodenz density-gradient separation (30, 51). Briefly, 1 g of soils were homogenized in 5 mL of 0.02% Tween 20 in phosphate-buffered saline (PBS) and vigorously vortexed for 30 min to detach microorganisms from soil particles. The soil slurry was further supplemented with 5 mL of 0.8 g/mL Nycodenz ($\geq 98\%$, Aladdin) solution and centrifuged at 10,000 rcf for 60 min. After centrifugation, the middle layer was carefully collected and transferred into a clean tube. The microorganisms from middle layer were washed three times with deionized water to remove residual PBS.

Single-Cell Raman Spectra Acquisition and Data Analysis. Soil bacteria were spotted on an aluminum-coated slide (HOOKE Instruments Ltd., China) and air dried at room temperature prior to Raman measurements. Single-cell Raman spectra were acquired using a LabRAM Aramis confocal Raman microscope (HORIBA Jonin-Yvon, Japan) with a 532 nm Nd:YAG laser (Laser Quantum) and 300 g/mm grating. A 100 \times objective (Olympus, Japan) was employed for Raman signal acquisition. The acquisition time of each cell was 15 s and the spectra were acquired in the range of 500–3,200 cm^{-1} . The C-D ratio of $\text{CD}/(\text{CD}+\text{CH})$ was used to indicate the degree of cellular D assimilation and calculated using the integration of spectral region assigned to C-D (2,040–2,300 cm^{-1}) and C-H vibrations (2,800–3,100 cm^{-1}). To calculate the abundance of D-labeled bacteria, more than 600 Raman spectra were obtained from each soil sample. The percentage of ARB was determined as the number of D-labeled bacteria identified by Raman- D_2O divided by the total number of single cells detected. The phenotypic resistance level was determined by multiplying the percentage and activity of ARB.

Single-Cell Sorting and Metagenomic Sequencing. The target bacteria that were highly labeled by D were sorted using a pulse laser ejection system one by one (PRECI SCS, HOOKE Instruments Ltd., China), and collected into a sterile receiver containing 2 μL of sterile PBS. Approximately 20 single cells were collected from each sorting process. A negative control without cell sorted (No sort) was also set in each treatment. The sorted cells were then transferred into cell lysis buffer, and the whole genomic DNA was amplified by multiple displacement amplification (MDA) following the protocol of REPLI-g single-cell Kit (Qiagen, Germany). MDA products were diluted 20 times in sterile water for bacterial 16S rRNA genes amplification using primers of 515F (GTGCCAGMCCGCGG) and 907R (CCGTAATCMTTTRAG) (52). PCR products of 16S rRNA genes were

visualized by an agarose gel electrophoresis. Only when the DNA samples from the sorted cells had positive PCR products and “No sort” control had no PCR products, these DNA were retained for metagenomic sequencing. A HiSeq system (Illumina Inc., San Diego, CA, USA) was used to perform the metagenomic sequencing at the Majorbio Bio-Pharm Technology Co., Ltd. (Shanghai, China).

Genome Assembly and Annotation. Twelve gigabases of sequencing data were generated for each sample. The sequencing reads were quality trimmed to eliminate reads less than 50 bp and average quality score lower than 30. The reads detected in the “No sort” control samples were filtered using Fastp v0.21.0. The remaining reads were assembled de novo using IDBA-UD v1.1.1 with default parameter (53). The genes in assembled contigs were predicted using Prodigal v2.6.3, and these genes were sought out from the NCBI NR database (02-2021) by using BLASTP v2.11.0 with the E-value $\leq 10^{-5}$. The contig sequences that had identities with nonbacterial sequences were removed. Only the genes on the bacterial contigs were annotated and those over 50% on the same taxon were annotated as the taxon (54). The initial binning of assembled contigs was performed using metaWRAP v1.3.2 (55) and checked for quality using CheckM v1.0.12 (56). The ARGs and VFGs-like genes were aligned to CARD and VFDB database respectively, using BLASTP with the E-value $\leq 10^{-5}$. The genes with at least 70% coverage and 80% similarity were identified as ARGs and VFGs. The abundance of each gene was calculated using the read counts of each predicted gene to compare sequencing depth and gene length, which were expressed as Reads Per Kilobase per Million mapped reads (RPKM) values (57). Marker genes from sorted *C. acnes* and 27 strains with a complete genome from NCBI database was used to build a phylogenetic tree. OrthoFinder v2.2.6 was used to infer rooted gene trees for all orthogroups (58), and the maximum likelihood tree was constructed using FastTree v2.1.10 (59), visualized with TreeDyn. MGEfinder was used to predict plasmid sequences for ARGs and VFGs-carrying contigs.

Soil DNA Extraction, 16S rRNA Gene Sequencing, and ARGs Determination. Soil DNA was extracted from 0.5 g fresh soil using the FastDNA Spin Kit for soil (MP Biomedical, Santa Ana, CA, USA). DNAs extracted from soils with and without antibiotics incubation were amplified by PCR using primers of F515 and 907R following the previously reported procedure (52). Illumina MiSeq platform was used to sequence PCR products at Meiji Biological Medicine Company, Shanghai, China. The raw data of 16S rRNA genes were assembled, quality-filtered, and analyzed in the QIIME (60). The operational taxonomic units (OTUs) were clustered via the UCLUST algorithm at a 97% sequence similarity (61). Taxonomic identification of bacteria was based on the Silva database (62). A total 285 ARGs were detected to reveal the effects of manure application on soil AMR by HT-qPCR (52). The HT-qPCR was performed using a Wafergen SmartChip real-time PCR system (Wafergen Inc., USA). Three technical repetitions were set in HT-qPCR. More details about the conditions of PCR amplification can be found in our previous studies (52).

Statistical Analyses. Shapiro-Wilks analysis was applied for normality test. One-way analysis of variance (ANOVA) and *t* test were employed to all statistical examination by using GraphPad Prism 5 and *P* value below 0.05 was considered significant. PCoA was used to assess the influence of antibiotics addition on soil microbial composition (Bray-Curtis distance). The differences in microbial community patterns were tested by permutational multivariate analysis of variance with the Adonis function (9,999 permutations).

Data, Materials, and Software Availability. All study data are included in the article and/or *SI Appendix*. Sequences have been deposited in the National Center for Biotechnology Information, Bio-Project: [PRJNA881589](https://www.ncbi.nlm.nih.gov/bioproject/PRJNA881589) (63).

ACKNOWLEDGMENTS. This work was supported by the National Natural Science Foundation of China (awards 21922608, 42021005, 22176186) and the Chinese Academy of Sciences (awards ZDBS-LY-DQC027).

1. C. Wilyard, The drug-resistant bacteria that pose the greatest health threats. *Nature* **543**, 15 (2017).
2. S. Hernando-Amado, T. M. Coque, F. Baquero, J. L. Martínez, Defining and combating antibiotic resistance from one health and global health perspectives. *Nat. Microbiol.* **4**, 1432–1442 (2019).
3. H. K. Allen *et al.*, Call of the wild: Antibiotic resistance genes in natural environments. *Nat. Rev. Microbiol.* **8**, 251–259 (2010).

4. D. H. Wall, U. N. Nielsen, J. Six, Soil biodiversity and human health. *Nature* **528**, 69–76 (2015).
5. N. Udikovic-Kolic, F. Wichmann, N. A. Broderick, J. Handelsman, Bloom of resident antibiotic-resistant bacteria in soil following manure fertilization. *Proc. Natl. Acad. Sci. U.S.A.* **111**, 15202–15207 (2014).

6. T. U. Berendonk *et al.*, Tackling antibiotic resistance: The environmental framework. *Nat. Rev. Microbiol.* **13**, 310–317 (2015).
7. Y. G. Zhu *et al.*, Diverse and abundant antibiotic resistance genes in Chinese swine farms. *Proc. Natl. Acad. Sci. U.S.A.* **110**, 3435–3440 (2013).
8. Q. L. Chen *et al.*, Application of struvite alters the antibiotic resistome in soil, rhizosphere, and phyllosphere. *Environ. Sci. Technol.* **51**, 8149–8157 (2017).
9. Q. L. Chen, H. L. Cui, J. Q. Su, J. Penuelas, Y. G. Zhu, Antibiotic resistomes in plant microbiomes. *Trends Plant Sci.* **24**, 530–541 (2019).
10. R. D. Bardgett, W. H. van der Putten, Belowground biodiversity and ecosystem functioning. *Nature* **515**, 505–511 (2014).
11. E. Singer, M. Wagner, T. Woyke, Capturing the genetic makeup of the active microbiome in situ. *ISME J.* **11**, 1949–1963 (2017).
12. U. Hofer, The majority is uncultured. *Nat. Rev. Microbiol.* **16**, 716–717 (2018).
13. K. G. Lloyd, A. D. Steen, J. Ladau, J. Yin, L. Crosby, Phylogenetically novel uncultured microbial cells dominate earth microbiomes. *mSystems* **3**, e00055-18 (2018).
14. B. Li *et al.*, Metagenomic and network analysis reveal wide distribution and co-occurrence of environmental antibiotic resistance genes. *ISME J.* **9**, 2490–2502 (2015).
15. T. S. Crofts, A. J. Gasparini, G. Dantas, Next-generation approaches to understand and combat the antibiotic resistome. *Nat. Rev. Microbiol.* **15**, 422–434 (2017).
16. P. Carini *et al.*, Relic DNA is abundant in soil and obscures estimates of soil microbial diversity. *Nat. Microbiol.* **2**, 16242 (2016).
17. E. Couradeau *et al.*, Probing the active fraction of soil microbiomes using BONCAT-FACS. *Nat. Commun.* **10**, 2770 (2019).
18. X. Zheng, C. Zong, M. Xu, X. Wang, B. Ren, Raman imaging from microscopy to nanoscopy, and to macroscopy. *Small* **11**, 3395–3406 (2015).
19. D. Berry *et al.*, Tracking heavy water (D₂O) incorporation for identifying and sorting active microbial cells. *Proc. Natl. Acad. Sci. U.S.A.* **112**, E194–E203 (2015).
20. K. Yang *et al.*, Rapid antibiotic susceptibility testing of pathogenic bacteria using heavy-water-labeled single-cell Raman spectroscopy in clinical samples. *Anal. Chem.* **91**, 6296–6303 (2019).
21. Y. Tao *et al.*, Metabolic-activity-based assessment of antimicrobial effects by D₂O-labeled single-cell raman microspectroscopy. *Anal. Chem.* **89**, 4108–4115 (2017).
22. D. Wang *et al.*, Advances in single cell Raman spectroscopy technologies for biological and environmental applications. *Curr. Opin. Biotechnol.* **64**, 218–229 (2020).
23. L. Cui *et al.*, Raman biosensor and molecular tools for integrated monitoring of pathogens and antimicrobial resistance in wastewater. *TrAC. Trends Anal. Chem.* **143**, 116415 (2021).
24. X. Zhang, A. L. Gillespie, A. L. Sessions, Large D/H variations in bacterial lipids reflect central metabolic pathways. *Proc. Natl. Acad. Sci. U.S.A.* **106**, 12580–12586 (2009).
25. M. Li, J. Xu, M. Romero-Gonzalez, S. A. Banwart, W. E. Huang, Single cell Raman spectroscopy for cell sorting and imaging. *Curr. Opin. Biotechnol.* **23**, 56–63 (2012).
26. K. S. Lee *et al.*, An automated Raman-based platform for the sorting of live cells by functional properties. *Nat. Microbiol.* **4**, 1035–1048 (2019).
27. X. Wang *et al.*, Positive dielectrophoresis-based Raman-activated droplet sorting for culture-free and label-free screening of enzyme function in vivo. *Sci. Adv.* **6**, eabb3521 (2020).
28. Y. Wang *et al.*, Raman-activated sorting of antibiotic-resistant bacteria in human gut microbiota. *Environ. Microbiol.* **22**, 2613–2624 (2020).
29. Y. Song *et al.*, Raman-deuterium isotope probing for in-situ identification of antimicrobial resistant bacteria in Thames River. *Sci. Rep.* **7**, 16648 (2017).
30. S. A. Eichorst *et al.*, Advancements in the application of NanoSIMS and Raman microspectroscopy to investigate the activity of microbial cells in soils. *FEMS Microbiol. Ecol.* **91**, fiv106 (2015).
31. M. Pan, L. M. Chu, Adsorption and degradation of five selected antibiotics in agricultural soil. *Sci. Total Environ.* **545–546**, 48–56 (2016).
32. J. B. Patel, F. Cockerill, P. A. Bradford, *Performance Standards for Antimicrobial Susceptibility Testing: Twenty-Fifth Informational Supplement* (Clinical and Laboratory Standards Institute, Wayne, PA, USA, 2015).
33. H.-Z. Li *et al.*, Phenotypic tracking of antibiotic resistance spread via transformation from environment to clinic by reverse D₂O single-cell raman probing. *Anal. Chem.* **92**, 15472–15479 (2020).
34. J. Q. Zhang, Y. H. Dong, Effect of low-molecular-weight organic acids on the adsorption of norfloxacin in typical variable charge soils of China. *J. Hazard. Mater.* **151**, 833–839 (2008).
35. Z. Fkova *et al.*, Microbial responses to selected pharmaceuticals in agricultural soils: Microcosm study on the roles of soil, treatment and time. *Soil Biol. Biochem.* **149**, 107924 (2020).
36. A. N. Zhang *et al.*, An omics-based framework for assessing the health risk of antimicrobial resistance genes. *Nat. Commun.* **12**, 4765 (2021).
37. D. G. J. Larsson, C. F. Flach, Antibiotic resistance in the environment. *Nat. Rev. Microbiol.* **20**, 257–269 (2022).
38. I. Zammit, R. B. M. Marano, V. Vaiano, E. Cytryn, L. Rizzo, Changes in antibiotic resistance gene levels in soil after irrigation with treated wastewater: A comparison between heterogeneous photocatalysis and chlorination. *Environ. Sci. Technol.* **54**, 7677–7686 (2020).
39. V. M. D'Costa *et al.*, Antibiotic resistance is ancient. *Nature* **477**, 457–461 (2011).
40. G. G. Zhan *et al.*, Comparative review of the carbapenems. *Drugs* **67**, 1027–1052 (2007).
41. P. C. Appelbaum, P. A. Hunter, The fluoroquinolone antibacterials: Past, present and future perspectives. *Int. J. Antimicrob. Agents* **16**, 5–15 (2000).
42. S. Pudasaini *et al.*, Microbial diversity of Browning Peninsula, Eastern Antarctica revealed using molecular and cultivation methods. *Front. Microbiol.* **8**, 591 (2017).
43. S. L. Berk, W. R. McCabe, Meningitis caused by gram-negative bacilli. *Ann. Intern. Med.* **93**, 253–260 (1980).
44. D. F. R. Doud *et al.*, Function-driven single-cell genomics uncovers cellulose-degrading bacteria from the rare biosphere. *ISME J.* **14**, 659–675 (2020).
45. S. H. Hwang, Y. J. Kim, Meropenem-resistant bacteria in hospital effluents in Seoul, Korea. *Environ. Monit. Assess.* **190**, 673 (2018).
46. Y. Che *et al.*, Mobile antibiotic resistome in wastewater treatment plants revealed by Nanopore metagenomic sequencing. *Microbiome* **7**, 44 (2019).
47. S. Yilmaz, M. Allgaier, P. Hugenholz, Multiple displacement amplification compromises quantitative analysis of metagenomes. *Nat. Methods* **7**, 943–944 (2010).
48. T. Xu *et al.*, Phenome-genome profiling of single bacterial cell by Raman-activated gravity-driven encapsulation and sequencing. *Small* **16**, e2001172 (2020).
49. S. Wagner *et al.*, Dissolved black carbon in throughfall and stemflow in a fire-managed longleaf pine woodland. *Biogeochemistry* **146**, 191–207 (2019).
50. T. Mitran, P. K. Mani, N. Basak, D. Mazumder, M. Roy, Long-term manuring and fertilization influence soil inorganic phosphorus transformation vis-a-vis rice yield in a rice-wheat cropping system. *Arch. Agron. Soil Sci.* **62**, 1–18 (2016).
51. H. Z. Li *et al.*, D₂O-isotope-labeling approach to probing phosphate-solubilizing bacteria in complex soil communities by single-cell Raman spectroscopy. *Anal. Chem.* **91**, 2239–2246 (2019).
52. Y.-G. Zhu *et al.*, Continental-scale pollution of estuaries with antibiotic resistance genes. *Nat. Microbiol.* **2**, 16270 (2017).
53. Y. Peng, H. C. Leung, S.-M. Yiu, F. Y. Chin, IDBA-UD: A de novo assembler for single-cell and metagenomic sequencing data with highly uneven depth. *Bioinformatics* **28**, 1420–1428 (2012).
54. S. Mitra *et al.*, Functional analysis of metagenomes and metatranscriptomes using SEED and KEGG. *BMC Bioinformatics* **12** (suppl. 1), S21 (2011).
55. G. V. Uritskiy, J. DiRuggiero, J. Taylor, MetaWRAP—a flexible pipeline for genome-resolved metagenomic data analysis. *Microbiome* **6**, 158 (2018).
56. D. H. Parks, M. Imelfort, C. T. Skennerton, P. Hugenholz, G. W. Tyson, CheckM: Assessing the quality of microbial genomes recovered from isolates, single cells, and metagenomes. *Genome Res.* **25**, 1043–1055 (2015).
57. A. Mortazavi, B. A. Williams, K. McCue, L. Schaeffer, B. Wold, Mapping and quantifying mammalian transcriptomes by RNA-Seq. *Nat. Methods* **5**, 621–628 (2008).
58. D. M. Emms, S. Kelly, OrthoFinder: Phylogenetic orthology inference for comparative genomics. *Genome Biol.* **20**, 238 (2019).
59. R. R. Core Team, *R: A Language and Environment for Statistical Computing* (R Foundation for Statistical Computing, Vienna, Austria, 2013).
60. J. G. Caporaso *et al.*, QIIME allows analysis of high-throughput community sequencing data. *Nat. Methods* **7**, 335–336 (2010).
61. R. C. Edgar, Search and clustering orders of magnitude faster than BLAST. *Bioinformatics* **26**, 2460–2461 (2010).
62. E. Pruesse *et al.*, SILVA: A comprehensive online resource for quality checked and aligned ribosomal RNA sequence data compatible with ARB. *Nucleic Acids Res.* **35**, 7188–7196 (2007).
63. Y.-G. Zhu *et al.*, To investigate antimicrobial resistance in soils. NCBI BioProject. <https://www.ncbi.nlm.nih.gov/bioproject/?term=PRJNA881589>. Deposited 17 September 2022.